ELSEVIER

Thermochimica Acta 386 (2002) 179–188

thermochimica acta

www.elsevier.com/locate/tca

Comparative study of the thermal decomposition of iron oxyhydroxides

Ivan Mitov*, Daniela Paneva, Boris Kunev

Institute of Catalysis, Bulgarian Academy of Sciences, "Acad. G. Bonchev" Str., Block 11, 1113 Sofia, Bulgaria

Received 8 May 2001; received in revised form 1 October 2001; accepted 8 October 2001

Abstract

The study is devoted to the thermal decomposition of the iron oxyhydroxides: γ-FeOOH (lepidocrocite), α-FeOOH (goethite) and $Fe_5HO_8{\cdot}4H_2O$ (ferrihydrite). The changes in the crystal structure, in the phase composition and in the dispersion degree, occurring during thermal treatment have been followed by means of Mössbauer spectroscopy, X-ray diffraction, infrared spectra, transmission electron microscopy (TEM), DTA/TG analysis and by measuring the specific surface area. The schemes of thermal dissociation of oxyhydroxides have been outlined on the basis of the obtained results. Some relaxation effects of nano-sized particles of the intermediate products have been observed in the course of this investigation and described respectively. Depending on the precursor, from which α-Fe_2O_3 has been obtained, it possesses various morphological (needle-like or spherical shape) and dispersion (particle size and specific surface area) features. The obtained results enable forecasts with respect to the optimal final product to be used as initial material for preparing heterogeneous catalysts and magnetic materials.

Keywords: Iron oxyhydroxides; Thermal decomposition; Mössbauer spectroscopy; X-ray

1. Introduction

The thermal treatment of precursors is important for the preparation of solid mixtures, such as heterogeneous catalysts, magnetic materials, pigments, etc. It usually follows the precipitation or mixing of the components and is especially important, since it determines the phase composition, crystal structure, ion distribution, dispersion, surface and crystallite and particles sizes.

In the literature, there is considerable experimental and theoretical material on the thermal decomposition of the different modifications of iron oxyhydroxides. The thermal decomposition of γ-FeOOH and the resulting products are the subject of several studies [1–6]. A series of transformations of lepidocrocite (γ-FeOOH) can also be observed either in suspensions of aqueous solutions of ferrosulphate [1] or during solid state temperature treatment, where a topotactic reaction accompanied by significant texture changes takes place [3]. It has been established that thermal treatment leads to crystal-chemical transformations according to the scheme γ-FeOOH → γ-Fe_2O_3 → α-Fe_2O_3 [5]. During the first step of the phase transformation sequence the crystallite size remains the same, whereas, during the second a drastic change in size is observed depending on the amount of water molecules in the initial lepidocrocite. The decrease of the specific surface area due to the water vapour partial pressure increase is discussed in [4].

There are a relatively large number of studies dealing with the thermal behaviour of α-FeOOH [6–13].

* Corresponding author. Fax: +359-2-756116.
E-mail address: mitov@ic.bas.bg (I. Mitov).

0040-6031/02/$ – see front matter
PII: S0040-6031(01)00808-5

All the previous studies have shown that the final product of the decomposition is α-Fe_2O_3, whose properties depend of the temperature of annealing [13], treatment conditions [7,11] and the crystallinity of the initial material [8].

Much attention has been paid [6,14–21] to the thermal behaviour of ferrihydrite ($Fe_5HO_8{\cdot}4H_2O$) and various gels which are considered to have formulas such as $Fe_5(O_4H_3)_3$, $Fe_2O_3{\cdot}2FeOOH{\cdot}xH_2O$. Various physicochemical methods have been used to study the heat effects [14], the intermediate phases [15] and the decomposition for which different schemes have been proposed [6,16,20]. The thermal stability, the dispersion of the final product and the corresponding spectra are described respectively in [17–19].

The problem under consideration here is associated with the formation of iron oxides in various media [1,24] and the effect of various additives [22,23] as well as with corrosion processes [25–28] during which crystal-chemical transformations analogous to those during thermal treatment are observed. The studies of iron oxyhydroxides and oxides phase transformations and the instrumental methods, applied therein, have been discussed in [29,30].

The publications in literature show that the dehydration process exhibits many characteristics that are common to a lot of polymorphous iron oxyhydroxides but there are also many differences.

The purpose of the present work is a comparative study of the thermal decomposition of γ-FeOOH, α-FeOOH and $Fe_5HO_8{\cdot}4H_2O$ under similar conditions.

2. Experimental

The two polymorphous FeOOH forms under consideration were prepared by oxidative hydrolysis of Fe(II) sulphate at $T = 273$ K, $C_{FeSO_4} = 20$ g/l for γ-FeOOH and $T = 333$ K, $C_{FeSO_4} = 150$ g/l for α-FeOOH. The ferrihydrite was synthesised by hydrolysis of Fe(III) sulphate at $T = 303$ K and $C_{Fe_2(SO_4)_3} = 150$ g/l. The hydrolysis of all samples proceeded at pH = 4.5. A detailed description of the preparation method and the properties of the iron oxyhydroxides obtained have been given in previous studies [31,32]. The applied method of synthesis and the chemical purity of the initial substances $Fe_2(SO_4)_3$ and $FeSO_4{\cdot}7H_2O$ from ''Merck'' gave phase pure γ-FeOOH, α-FeOOH and $Fe_5HO_8{\cdot}4H_2O$. The temperatures of thermal annealing were selected on the basis of observed heat effects by the DTA/TG.

The Mössbauer spectra were obtained at room temperature with a Wissel (Wissenschaftliche Elektronik GmbH, Germany) electromechanical spectrometer working in a constant acceleration mode. A ^{57}Co/Cr (activity ≅ 20 mCi) source and an α-Fe standard were used. The experimentally obtained spectra were subjected to mathematical processing according to the least squares method. Phase identification was made by X-ray diffraction (TUR-M62 apparatus, Germany, equipped with a computer-directed HZG-4 goniometer with Co Kα radiation). Diffraction line profile analysis was performed by the program developed in [33]. The mean crystallite size was determined

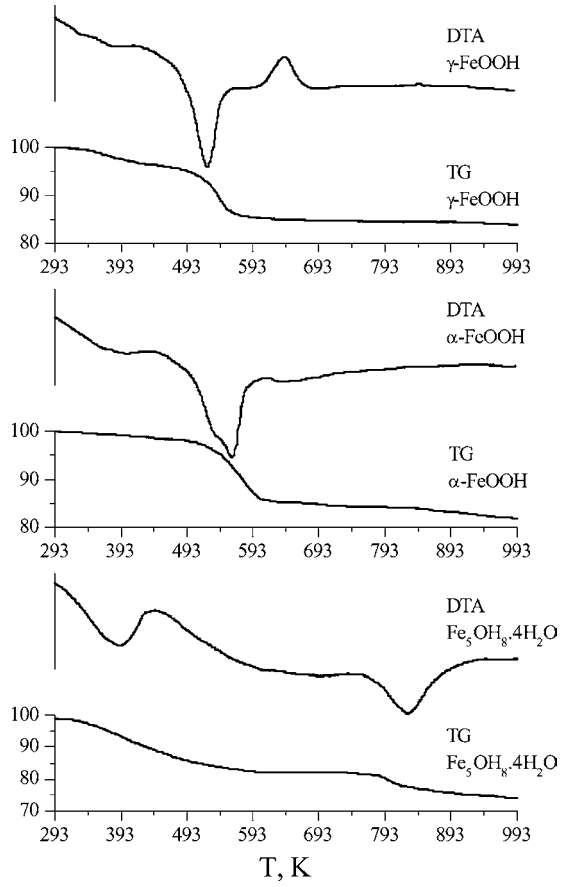

Fig. 1. DTA/TG curves of γ-FeOOH, α-FeOOH and $Fe_5HO_8{\cdot}4H_2O$.

from the width of the Lorentzian component. The infrared spectra were obtained with a Bruker IFS-25 apparatus (Germany). The DTA analysis was carried out with a Derivatograph-1500 apparatus (Hungary). Electron microscope pictures of the initial and final products were taken with a JEM-100B apparatus (Japan). The specific surface area was determined by the BET method.

Table 1
Weight loss of γ-FeOOH, α-FeOOH and $Fe_5HO_8{\cdot}4H_2O$ determined by TG at different temperature intervals

Sample	Percentage of initial weight (±0.2)		
	300–423 K	300–623 K	300–993 K
γ-FeOOH	3.4	15.0	16.2
α-FeOOH	1.2	14.8	18.3
$Fe_5HO_8{\cdot}4H_2O$	9.3	17.8	26.1

3. Results and discussion

The infrared spectra of the samples indicate pure phases of γ-FeOOH, α-FeOOH and $Fe_5HO_8{\cdot}4H_2O$ [6,13,23,34,35]. The spectra of the initial samples of α-FeOOH and γ-FeOOH are characterised by narrow and intensive bands, which is indicative of well-crystallised samples [23,34]. Comparison of the area ratio of OH^- and Fe–O stretching modes for the three oxyhydroxides shows the highest OH^- content in the

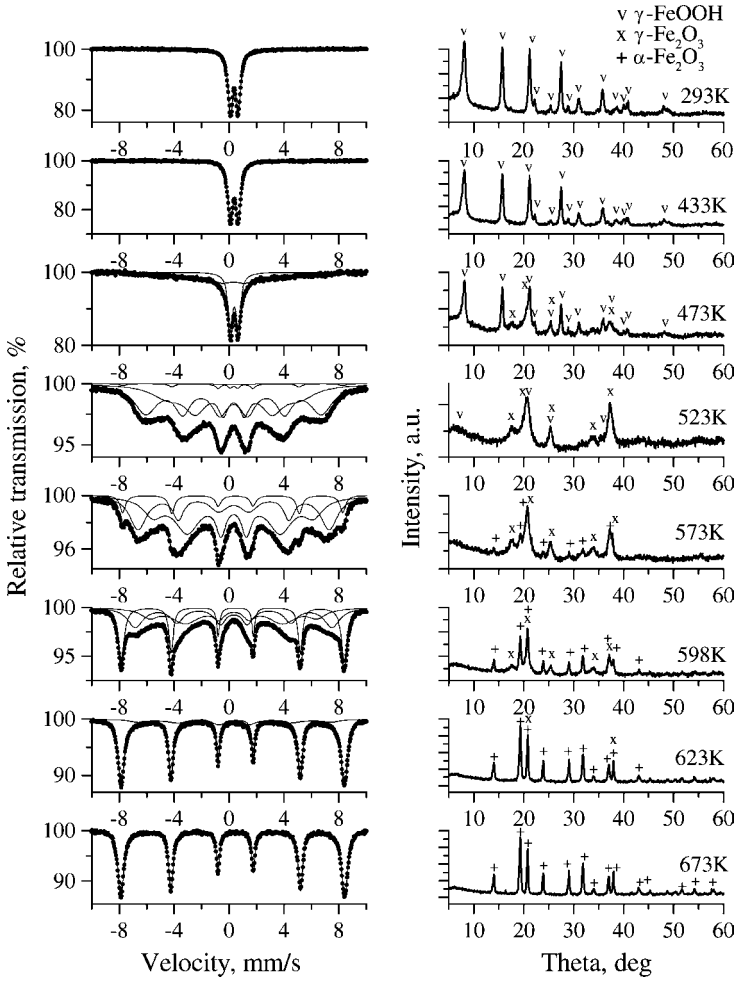

Fig. 2. Mössbauer spectra and X-ray diffractograms of initial γ-FeOOH and heat-treated samples at $T = 293-673$ K.

ferrihydrite, which is in qualitative agreement with [35].

The characteristic heat effects as determined from the DTA/TG curves (Fig. 1) are the following:

- γ-FeOOH: A weak endothermic effect within the temperature range 353–403 K, a strong endothermic effect at 453–600 K and an exothermic effect at 613–753 K.
- α-FeOOH: A weak endothermic effect at 410 K, a shoulder of an endothermic effect at 553 K and an endothermic effect at 553–673 K.
- $Fe_5HO_8{\cdot}4H_2O$: An endothermic effect at 393 K, a diffuse endothermic effect at 473–773 K, a weak exothermic effect at 773 K and an endothermic effect at 830 K.

The TG curves are also presented in Fig. 1. Table 1 shows the weight loss at different temperatures. From the weight loss one may find the general formulas of the oxyhydroxides under consideration: γ-FeOOH·$0.17H_2O$, α-FeOOH·$0.05H_2O$ and $Fe_5HO_8{\cdot}2.48H_2O$. The water is probably absorbed during storage of the samples in air.

All endothermic effects can be ascribed to dehydration of the oxyhydroxides. In the case of α-FeOOH the two endothermic effects are due to goethite dehydration hindered by the formation of a surface layer of hematite [7]. The exothermic effect of γ-FeOOH is due to the $\gamma\text{-}Fe_2O_3 \rightarrow \alpha\text{-}Fe_2O_3$ transition.

The Mössbauer and X-ray diffraction spectra of the γ-FeOOH initial and heat-treated samples are shown in Fig. 2. The Mössbauer parameters of hyperfine interaction, such as isomer shift (IS), quadrupole splitting (QS) and effective internal magnetic field (H_{eff}) as well as the line widths (FWHM) and the relative area (A) of the phases observed at different temperatures of annealing are given in Table 2.

The Mössbauer spectra and parameters identify the scheme of dehydration and decomposition of γ-FeOOH. Up to 433 K, physically-bonded water only is evolved and the Mössbauer spectrum consists of a quadrupole doublet. Disturbance of the symmetry of electrical charges around the iron nucleus results in a negligible increase in QS. At 473 K, formation of $\gamma\text{-}Fe_2O_3$ is registered by the appearance of a sextet with unresolved lines. With rising temperature the nano-sized particles of the maghemite increase and

Table 2
Mössbauer parameters of heat-treated sample γ-FeOOH

Temperature (K)	Phase composition	IS (mm/s) (±0.007)	QS (mm/s) (±0.006)	H_{eff} (kOe) (±3)	A (%) (±2)
293	γ-FeOOH	0.379	0.565	–	100
433	γ-FeOOH	0.380	0.574	–	100
473	γ-FeOOH	0.379	0.574	–	42
	$\gamma\text{-}Fe_2O_3$(SPM)	0.319	−0.002	343	58
523	γ-FeOOH	0.355	0.570	–	0.7
	$\gamma\text{-}Fe_2O_3$(A)	0.326	−0.004	398	54
	$\gamma\text{-}Fe_2O_3$(B)	0.326	−0.013	300	43
	$\alpha\text{-}Fe_2O_3$	0.360	−0.100	498	2.3
573	$\gamma\text{-}Fe_2O_3$(A)	0.335	−0.001	432	35
	$\gamma\text{-}Fe_2O_3$(B)	0.313	−0.017	364	57
	$\alpha\text{-}Fe_2O_3$	0.376	−0.109	499	8
598	$\gamma\text{-}Fe_2O_3$(A)	0.344	−0.007	446	29
	$\gamma\text{-}Fe_2O_3$(B)	0.332	−0.013	381	40
	$\alpha\text{-}Fe_2O_3$	0.380	−0.105	505	31
623	$\alpha\text{-}Fe_2O_3$	0.380	−0.103	505	81
	$\gamma\text{-}Fe_2O_3$	0.336	0.013	438	19
673	$\alpha\text{-}Fe_2O_3$	0.378	−0.104	508	99.8
	$\gamma\text{-}Fe_2O_3$ trace	0.356	0.002	495	<0.2

high-dispersity γ-Fe_2O_3 is formed. Aggregates of different size are formed and are denoted as γ-Fe_2O_3(A) and γ-Fe_2O_3(B), respectively. The γ-Fe_2O_3(A) has a smaller relative fraction, consisting of larger particles, whereas, γ-Fe_2O_3(B) has a larger relative fraction, consisting of smaller particles (Table 2). The highly dispersed maghemite differs in its QS values from a well-crystallised standard of the same substance. The smaller the maghemite particles, the higher the QS value. The presence of QS is an indication of disturbed local symmetry of the neighbours around the iron nucleus. The appearance of intense hematite lines is observed at 598 K, which indicates a γ-$Fe_2O_3 \rightarrow$ α-Fe_2O_3 transition. Above 673 K the main phase shown by the spectrum is α-Fe_2O_3 along with traces of γ-Fe_2O_3. The latter is ferromagnetic. Above this temperature the spectrum is practically a single-component one—there is only α-Fe_2O_3.

The diffraction spectra (Fig. 2) confirm the above Mössbauer results. The succession of the crystal-chemical transformations from the initial γ-FeOOH to γ-Fe_2O_3 having nano-sized crystallites and their transformation into α-Fe_2O_3 has been proved. The mean crystallite sizes determined from these spectra range from 8 to 20 nm for the initial γ-FeOOH and from 50–120 nm for the resulting α-Fe_2O_3. The "contradiction" between the Mössbauer and X-ray spectra of the samples heated at 523 and 573 K should be noted.

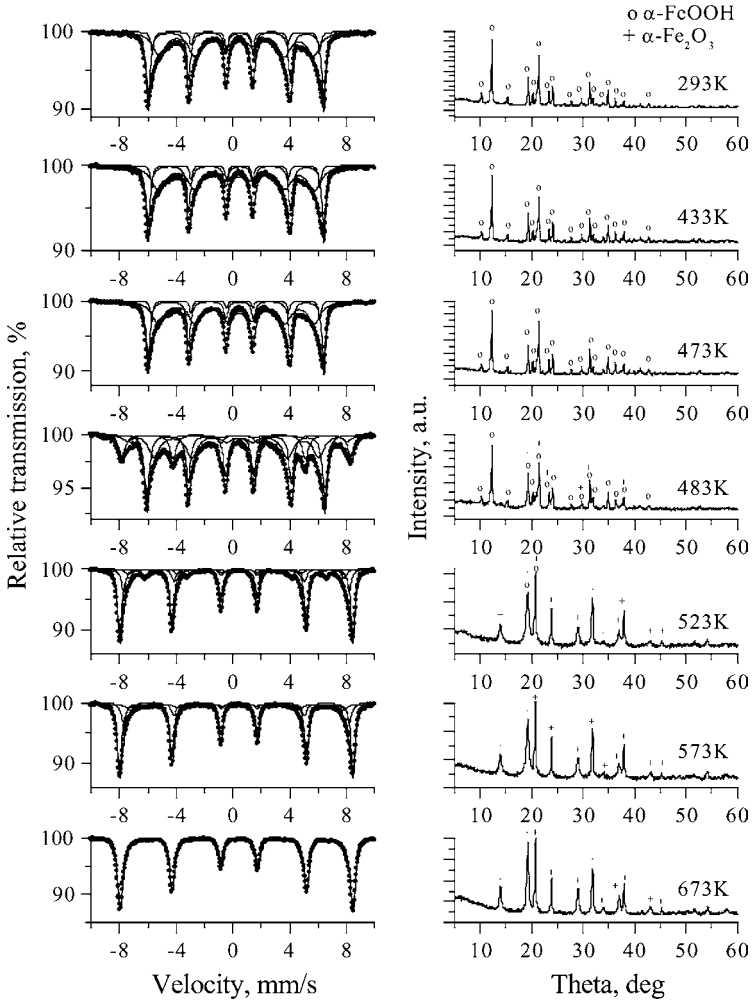

Fig. 3. Mössbauer spectra and X-ray diffractograms of initial α-FeOOH and heat-treated samples at $T = 293-673$ K.

The crystallite size of high-dispersity maghemite as determined from the diffraction spectra is 3–4 nm. The Mössbauer spectra corresponding to these sizes should be quadrupole doublets reflecting a superparamagnetic (SPM) effect. However, the experimental spectra contain sextuplets, although with very low H_{eff} values (the values for the internal magnetic field are distributed between 280 and 400 kOe), along with broad lines. These results may be interpreted within the framework of the model of inter-particle interaction described by Tronc and Bonnin [36]. This interaction leads to the so-called effect of superferromagnetism (SFM). The same authors has also described [37] a magnetic coupling of a spinel type iron oxide in a cationic sol flocculated by different agents. The SFM effect is due to magnetic coupling of the particles, which form packs. This leads to an increase of the total volume of coupled particles. As a result, the frequency of heat relaxation of the magnetic vector direction decreases. The Mössbauer spectrum of packs of coupled particles exceeding the critical size (10–12 nm) will register hyperfine magnetic interaction by the appearance of sextets. The factors leading to this ''magnetic coupling'' are a magnetic dipole interaction between crystal needles and exchange interactions between ion couples situated on the surface of different particles. There are good reasons to assume the larger contribution to belong to the second kind of interactions. Hence, the results from the diffraction spectra can be considered as an indication of the crystallite sizes while the Mössbauer spectra give information on the size of crystallite aggregates.

The Mössbauer spectra and X-ray diffractograms of heat-treated samples of α-FeOOH are given in Fig. 3. The spectra of this oxyhydroxide (initial samples have crystallite sizes in the range 25 to 125 nm), display new Mössbauer and diffraction lines due to thermal decomposition at 483 K. Complete decomposition is achieved at 573 K. The product obtained initially is highly disperse Fe_2O_3 with reduced H_{eff} values (the magnetic field is distributed within the limits of $H_{eff} = 480-505$ kOe) and broad lines. After heating at 673 K, a better crystallised α-Fe_2O_3 is obtained (crystallite sizes ranging from 30 to 250 nm). The

Table 3
Mössbauer parameters of heat-treated sample α-FeOOH

Temperature (K)	Phase composition	IS (mm/s) (±0.007)	QS (mm/s) (±0.006)	H_{eff} (kOe) (±3)	A (%) (±3)
293	α-FeOOH(A)	0.350	−0.132	386	39
	α-FeOOH(B)	0.349	−0.134	366	11
	α-FeOOH(C)	0.354	−0.119	338	50
433	α-FeOOH(A)	0.350	−0.132	386	37
	α-FeOOH(B)	0.347	−0.137	369	10
	α-FeOOH(C)	0.354	−0.115	345	53
473	α-FeOOH(A)	0.348	−0.132	386	37
	α-FeOOH(B)	0.346	−0.138	369	8
	α-FeOOH(C)	0.353	−0.118	343	55
483	α-FeOOH(A)	0.351	−0.134	391	42
	α-FeOOH(B)	0.356	−0.112	362	31
	α-Fe_2O_3(A)	0.348	−0.102	502	19
	α-Fe_2O_3(B)	0.311	−0.098	482	8
523	α-Fe_2O_3(A)	0.354	−0.105	512	63
	α-Fe_2O_3(B)	0.348	−0.104	496	17
	α-Fe_2O_3(C)	0.352	−0.090	471	10
	α-FeOOH	0.351	−0.118	396	10
573	α-Fe_2O_3(A)	0.355	−0.106	512	69
	α-Fe_2O_3(B)	0.345	−0.099	496	18
	α-Fe_2O_3(C)	0.353	−0.087	466	13
673	α-Fe_2O_3	0.372	−0.103	512	100

change in ratio of the intensities of some diffraction lines can be attributed to anisotropy in the crystallite ordering. Amorphous intermediates have not been observed, as has been pointed out in a previous study [11]. The Mössbauer parameters for the different phases present at different temperatures of annealing are given in Fig. 3 and Table 3. The indexes in brackets (A, B and C) following the formulas α-FeOOH and α-Fe_2O_3 denote different particle sizes. The index A denotes the particles with the greatest size and C those with the smallest size.

The Mössbauer spectra do not show the presence of phases with SPM or SFM behaviour similar to that observed during dehydration of the same samples prepared by mechano-chemical activation [38].

Using the same polymorphous form of iron oxyhydroxide (α-FeOOH), however, obtained after oxidative hydrolysis at $T = 303$ K, we performed spectral studies after the thermal decomposition of the oxyhydroxide (Fig. 4). This sample consists particles of different sizes including such ones that have SPM properties at room temperature.

The initial spectrum (approximated as three sextets and one quadrupole doublet) shows that four groups of aggregates can be determined on the basis of their sizes. The fraction of the small particles (below 12 nm) is 10%. After heating at 433 K the SPM component vanishes and the spectrum is almost the same as that of the sample, obtained at $T = 333$ K. The increase in dispersion of the intermediate products as a result of the improved dispersion of the initial substance is less than expected.

The Mössbauer spectra and X-ray diffractograms of thermal decomposition of $Fe_5HO_8{\cdot}4H_2O$ (mean crystallite size 3 nm) are shown in Fig. 5. The spectra include doublet components which are preserved up to 748 K and sextet components appearing at the same temperature. Heating at 573 K does not change the spectra. Only an increase in the QS values from 0.74 to 0.85 mm/s (Table 4) is observed and attributed to a change in symmetry around the iron nucleus due to partial evolution of the crystal water. After treatment at 673–723 K, both the X-ray and Mössbauer spectra exhibit new lines similar to those of hematite (crystallite size 4 nm). According to [21], the product obtained is hydrohematite in which the OH^- groups are assumed to occupy the anionic position in the dense packing of the anionic sub-lattice of hematite.

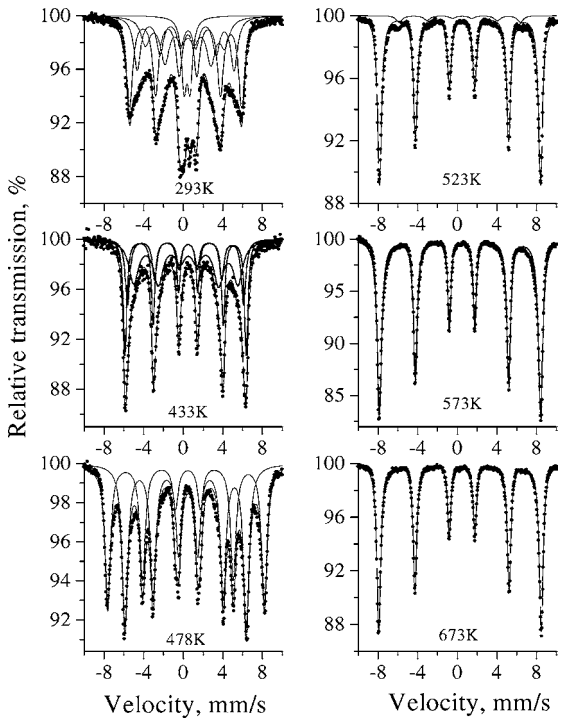

Fig. 4. Mössbauer spectra of high dispersed initial α-FeOOH and heat-treated samples at $T = 293-673$ K.

The suggestion about the formation of hydrohematite is also supported by the fact that the large loss of weight has not occurred yet (Table 1) and the weak exothermic effect at 773 K of α-Fe_2O_3 crystallisation is not yet observable. The spectrum of hydrohematite is a SPM doublet which is preserved up to $T = 748$ K. Further dehydration leads to the formation of α-Fe_2O_3 of various dispersion: α-Fe_2O_3(A) refers to lower dispersion and α-Fe_2O_3(B) to higher dispersion, both having low values of H_{eff} ($H_{\text{eff}} = 460-510$ kOe). After heating at 823 K, the α-Fe_2O_3 formed is characterised with $H_{\text{eff}} = 516$ kOe (Table 4). The mean crystallite size of the final product is about 15 nm. Due to the different preparation method of the initial sample as compared to that of the sample described in [20], there is a difference in evolution of the ferrihydrite during thermal treatment.

The data from transmission electron microscopy (TEM) are also in agreement with the above spectral analysis. The crystals of the initial γ- and α-FeOOH have the shape of needles. The values of the crystallite sizes are higher than those obtained from the

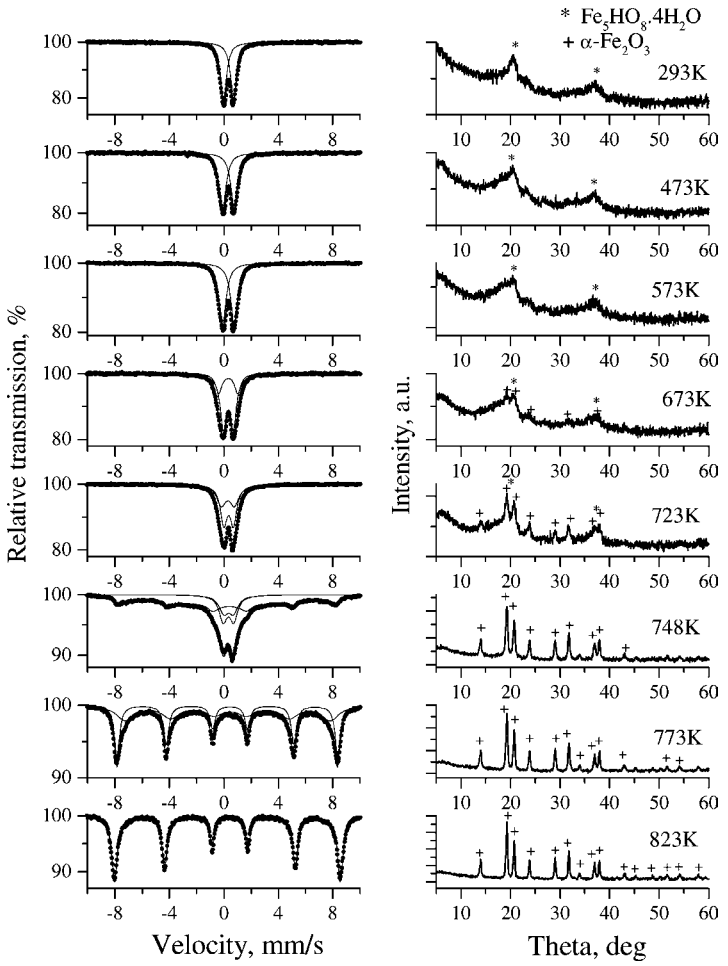

Fig. 5. Mössbauer spectra and X-ray diffractograms of initial $Fe_5HO_8{\cdot}4H_2O$ and heat-treated samples at $T = 293-823$ K.

Table 4
Mössbauer parameters of heat-treated sample $Fe_5HO_8{\cdot}4H_2O$

Temperature (K)	Phase composition	IS (mm/s) (±0.007)	QS (mm/s) (±0.006)	H_{eff} (kOe) (±2)	A (%) (±3)
293	$Fe_5HO_8{\cdot}4H_2O$	0.337	0.743	–	100
473	$Fe_5HO_8{\cdot}4H_2O$	0.329	0.844	–	100
573	$Fe_5HO_8{\cdot}4H_2O$	0.326	0.858	–	100
673	$Fe_5HO_8{\cdot}4H_2O$	0.327	0.743	–	73
	α-Fe_2O_3(SPM)	0.321	1.406	–	27
723	$Fe_5HO_8{\cdot}4H_2O$	0.354	0.720	–	50
	α-Fe_2O_3(SPM)	0.283	0.921	–	50
748	α-Fe_2O_3	0.342	−0.101	493	65
	α-Fe_2O_3(SPM)	0.332	0.782	–	20
	$Fe_5HO_8{\cdot}4H_2O$	0.346	0.723	–	15
773	α-Fe_2O_3(A)	0.351	−0.103	504	49
	α-Fe_2O_3(B)	0.358	−0.092	468	51
823	α-Fe_2O_3	0.355	−0.094	516	100

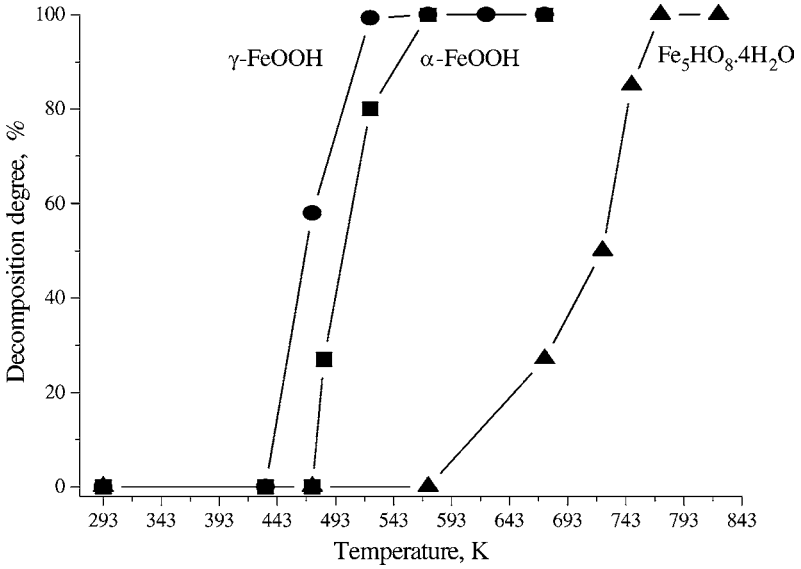

Fig. 6. Temperature dependence of thermal decomposition degree of γ-FeOOH, α-FeOOH and $Fe_5HO_8{\cdot}4H_2O$.

diffraction spectra. This difference is due to the different determination methods. The crystallites observed by TEM contain microcracks, which broadens the diffraction lines. An additional proof in this respect if the presence of a Gaussian component in the diffraction lines, which amounts to 20% of the line area. The crystallite sizes as determined by TEM are: mean width 15 nm, mean length 60 nm for γ-FeOOH; mean width 30 nm, mean length 250 nm for α-FeOOH. The crystallites preserve their shape and represent needles in the final α-Fe_2O_3. Only an increase in size and a decrease in the length/width ratio of the crystallites are observed.

The initial ferrihydrite sample consists of almost amorphous agglomerates whose particles have mean sizes of 4–5 nm and a spherical shape. The same picture is also observed after thermal treatment when the crystalline hematite represents a mass of fine crystallites coalescing to grains with irregular shapes and no orientation.

Table 5
Specific area of the samples γ-FeOOH, α-FeOOH and $Fe_5HO_8{\cdot}4H_2O$

Sample	Specific area (m^2/g) (±4)
Initial sample γ-FeOOH	124
α-Fe_2O_3 obtained from γ-FeOOH	28
Initial sample α-FeOOH	107
α-Fe_2O_3 obtained from α-FeOOH	17
Initial sample $Fe_5HO_8{\cdot}4H_2O$	160
α-Fe_2O_3 obtained from $Fe_5HO_8{\cdot}4H_2O$	42

Additional information can also be obtained from the measured specific surface areas (Table 5). The largest specific surface area belongs to the product of ferrihydrite thermal dissociation. The thermal decomposition dynamics of the different polymorphous forms of iron oxyhydroxide can be seen in Fig. 6. The degree of decomposition is determined by the relative fractions of the components in Mössbauer spectra for oxyhydroxide samples heated at the selected temperatures.

The figure shows that under analogous conditions of thermal treatment, γ-FeOOH dehydration is faster than that of α-FeOOH and the two oxyhydroxides are dehydrated at temperatures much lower than that of $Fe_5HO_8{\cdot}4H_2O$.

4. Conclusions

The present comparative study of the thermal decomposition of various polymorphous iron oxyhydroxide shows that their dehydration proceeds at

different temperatures. There are differences in the stages of dehydration and decomposition as well as in the intermediate products. The final dehydration product is α-Fe_2O_3 which, depending on the precursor, has different morphological and dispersion characteristics.

On the basis of the results obtained, a preliminary estimation of the qualities of α-Fe_2O_3 prepared from different precursors can be made with a view to its use as a basis of iron-containing catalysts. The product obtained from lepidocrocite, containing ferromagnetic maghemite admixture, is the most unsuitable one because of the residual ferromagnetism, which could cause some technological difficulties. In this sense the hematite obtained from goethite and ferrihydrite seems to be more promising. The α-Fe_2O_3 prepared by decomposition of ferrihydrite has a more pronounced dispersion. Even above 623 K, this product has hydroxyl groups which may participate in the catalytic reaction.

References

[1] K. Bechine, J. Subrt, T. Hanslik, V. Zapletal, J. Tlaskal, J. Lipka, B. Sedlak, M. Rotter, Z. Anorg. Allg. Chem. 489 (1982) 186.
[2] H. Watanabe, J. Seto, Bull. Chem. Soc. Jpn. 66 (1993) 395.
[3] H. Naono, K. Nakai, J. Colloid Interface Sci. 128 (1989)146.
[4] D.G. Klissurski, J. Subrt, V.N. Blaskov, J. Lipka, P. Hanousek, K. Bechine, J. Mater. Sci. 19 (1984) 183.
[5] P.M.A. de Bakker, E. de Grave, R.E. Vandenberghe, L.H. Bowen, R.J. Pollard, R.M. Persoons, Phys. Chem. Miner. 18 (1991) 131.
[6] U. Schwertmann, R.M. Cornell, Iron Oxide in the Laboratory, VCH, Weinheim, 1991, p. 61.
[7] R. Derie, M. Ghodsi, C. Calvo-Roche, J. Thermal Anal. 9 (1976) 435.
[8] S. Goni-Elizalde, M.E. Garcia-Clavel, Thermochim. Acta 124 (1988) 359.
[9] V.I. Kuznetsov, O.P. Krivoruchko, E.N. Yurchenko, E.A. Taraban, R.A. Buyanov, M.T. Protasova, G.N. Kryukova, Izv. SO AN SSSR Ser. Him. Nauk. 1 (1986) 36.
[10] E. Mendelovici, R. Villalba, A. Sagarzazu, Mater. Res. Bull. 17 (1982) 241.
[11] D.G. Klissurski, V.N. Bluskov, Mater. Chem. 5 (1980) 67.
[12] N.V. Murashko, A.V. Baranov, E.I. Petuhov, Izv. AN SSSR Neorganicheskie Materialy Russ. 16 (1980) 1244.
[13] A.Y. Vlasov, G.V. Loseva, G.S. Sakash, L.S. Solntseva, Zh. Prikl. Spektrosk. Russ. 12 (1970) 1130.
[14] S. Rajendran, V. Sitakara Rao, H.S. Maiti, J. Mater. Sci. 17 (1982) 2709.
[15] L. Markov, V. Blaskov, D. Klissurski, S. Nikolov, J. Mater. Sci. 25 (1990) 3096.
[16] S.V.S. Prasad, V. Sitakara Rao, J. Mater. Sci. 19 (1984) 3266.
[17] H. Stanjek, P.G. Weidler, Clay Miner. 27 (1992) 397.
[18] F.V. Chukhrov, B.B. Zvyagin, A.I. Gorshkov, L.P. Ermilova, V.V. Balashova, Izv. Acad. Nauk. SSSR Ser. Geol. Russ. 4 (1973) 23.
[19] E. Murad, U. Schwertmann, Am. Miner. 65 (1980) 1044.
[20] E.V. Pashkova, E.B. Novosadova, V.P. Chalii, V.P. Ivanitskii, P.O. Voznuk, Ukrainski Kim. Zh. Russ. 51 (1985) 244.
[21] E. Wolska, Z. Kristallogr. 154 (1981) 69.
[22] N.J. Reeves, S. Mann, J. Chem. Soc. Faraday Trans. 87 (1991) 3875.
[23] G.S.R. Krishnamurti, P.M. Huang, Clays Clay Miner. 39 (1991) 28.
[24] J. Pattanayak, V. Sitakara Rao, H.S. Maiti, J. Mater. Sci. 25 (1990) 2245.
[25] G. Belozerskii, C. Bohm, T. Ekdahl, D. Liljequist, Corros. Sci. 22 (1982) 831.
[26] A.A. Olowe, J.M.R. Genin, Hyperfine Interactions 46 (1989) 445.
[27] M. Stratmann, K. Hoffmann, Corros. Sci. 29 (1989) 1329.
[28] B. Kounde, A. Raharinaivo, A.A. Olowe, D. Rezel, Ph. Bauer, J.M.R. Genin, Hyperfine Interactions 46 (1989) 421.
[29] E. Murad, Hyperfine Interactions 47 (1989) 33.
[30] G. Long, J. Stevens, Industrial Application of the Mössbauer Effect, Plenum Press, New York, 1986, p. 63.
[31] D. Andreeva, T. Tabacova, I. Mitov, A. Andreev, J. Mater. Sci. Mater. Electron. 2 (1991) 199.
[32] I. Mitov, T. Tabacova, D. Andreeva, T. Tomov, Z. Phys. D Atoms Mol. Clusters 19 (1991) 275.
[33] V. Petkov, N. Bakaltchev, J. Appl. Cryst. 23 (1990) 138.
[34] S. Goni-Elizalde, M.E. Garcia-Clavel, J. Am. Ceram. Soc. 73 (1990) 121.
[35] J.D. Russell, Clay Miner. 14 (1979) 109.
[36] E. Tronc, D. Bonnin, J. Phys. Lett. 46 (1985) L437.
[37] E. Tronc, J.P. Jolivet, Hyperfine Interactions 28 (1986) 525.
[38] I. Mitov, V. Mitrov, J. Mechanochem. Mech. Alloying 1 (1994) 159.